Delft University of Technology

A model for controlled dosing of femto-litre volume liquids using hollow microcantilever

Cao, Xi; Gruiter, Rick de; van Oorschot, Ralph; Baldi, Simone; Hossein Nia Kani, Hassan; Ghatkesar, Murali Krishna

Important note
To cite this publication, please use the final published version (if applicable).
Please check the document version above.

A model for controlled dosing of femto-litre volume liquids using hollow microcantilever

Xi Cao[1,*], Rick de Gruiter[2], Ralph van Oorschot[3],
Simone Baldi[1], Hassan HosseinNia[2],
Murali Krishna Ghatkesar[2,**]

[1] Delft Center for Systems and Control, Delft University of Technology, The Netherlands,
[2] Precision and Microsystems Engineering, Delft University of Technology, The Netherlands,
[3] MA3 Solutions B.V., Eindhoven, The Netherlands.
*X.Cao-4@student.tudelft.nl; **M.K.Ghatkesar@tudelft.nl

Abstract: A hollow microcantilever is used instead of a conventional microcantilever to dispense and aspirate liquids in the femto-litre (10^{-15} L) volume range in an atomic force microscope (AFM) setup. The inherent force sensing capability of the cantilever is used to monitor the fluid manipulation in-situ. At this small scale, parameters like: surface energy, evaporation, viscosity and temperature become important for controlled manipulation. In a conventional AFM, these parameters are usually not taken into consideration as feedback parameters. In the present work, we report initial experimental results on the dosing process and an analytical dynamic model of the process. The model is based on the liquid bridge between the cantilever tip and the substrate, which can describe the dosing process with variance accounted for (VAF) larger than 90%. We aim to use this model and implement a control system for precise dispensing and aspiration.

Keywords: dynamic modelling, hollow-cantilever, nanotechnology, femto-liter, Atomic Force Microscope

1. INTRODUCTION

Nanotechnology has been first introduced by Richard Feynman in 1959. In 1990s, the interest in nanotechnology greatly increased (Elnashaie et al. (2015)), and nowdays, a lot of branches in nanotechnology have arisen: handling liquids at nanoscale is one of them, with applications in surface nanopatterning or molecules deposition on surfaces. Atomic force microscope (AFM) has become a crucial enabler of dosing liquids in the order of femtoliter. Three different types of AFM-based tools are used for dosing liquids at the femtoliter scale (Ghatkesar et al. (2014)): the first one is the chip without reservoir, called as DPN (Dip Pen Nanolithography). The second one is the chip with a reservoir just above the tip of AFM (hollow tip), called as NADIS (Nanoscale Dispensing). The third one is the chip with a reservoir: the liquid can flow from on-chip reservoir through the hollow cantilever and dispensed from the aperture at the tip, such as AFM-FP (atomic force microscope femto pipette) and NFProbe (Nanofountain Probe). The hollow cantilever AFM has the advantage that it could both aspirate and dispense liquids, if connected with a pressure control system. So it opens the possibility to control the dosing process *dynamics* via a properly designed applied pressure. However, a dynamic model is the necessary first step for the initiation of such control system. The goal of this work is modeling the *dosing dynamics* happening in an AFM-FP.

The first contribution of this work arises from the fact that while the state of the art provides us only with experimental data and empirical analysis about factors influencing the dispensing process of NADIS and DPN (Fabié et al. (2009); OConnell et al. (2014)), in this paper, a dynamic model of the dosing process is formulated for the first time. Two principles (Laplace pressure and electrical circuit analogy method) are appropriately combined to develop the dynamic model.

The second contribution of this work is the validation of the dynamic model, via a set of appropriately designed dosing experiments: it is demonstrated that the proposed model can describe the dosing process with variance accounted for (VAF) larger than 90%. VAF is used to assess the quality of a model, which is defined as:

$$VAF = (1 - \frac{\frac{1}{N}\sum_{k=1}^{N} \|y(k) - y_m((k))\|_2^2}{\frac{1}{N}\sum_{k=1}^{N} \|y(k)\|_2^2}) \times 100\%$$

where $y(k)$ is the experimental data and $y_m(k)$ is the data from model. VAF values close to 100% indicates that the model is a good representation of the physical process.

The rest of the paper is organized as follows. Section 2 introduces the dosing process. Section 3 explains the modeling steps. In Section 4 experimental methods to measure volume and contact angle are explained. Experimental results with model validation are illustrated in Section 5. Section 6 concludes the paper and discusses future work.

2. THE DOSING PROCESS

"Dosing" means putting a desired volume of liquids in a specific position of the substrate by dispensing and aspirating. The dosing device comprises AFM-FP, climate control system and pressure control system (van Oorschot et al. (2015)). The dosing process steps are shown Figure 1. The corresponding cantilever deflection signal monitored with distance above the substrate surface is shown in Figure 2.

In step 1, the hollow cantilever approaches the substrate with a constant *step size*. It is the distance which the hollow cantilever AFM tip moves vertically in a specific period.

In step 2, the tip touches the substrate, and the external pressure control system provides pressure for a certain period. The position where the tip first touches the substrate is the *snap in* position. The blue line in Figure 2 represents the signal from step 1 and step 2. The contact period is called *contact time*. And the liquid connecting tip and substrate is called *liquid bridge*.

In step 3, the tip starts to retract from the substrate at the same step size. After the liquid bridge breaks up, the liquid droplet remains on the substrate, which represent the step 4 of the process. The red line in Figure 2 represents the signal from step 3 and step 4.

The *contact angle* β (rad) is measured through the liquid, where a liquid-vapor interface meets a solid surface. In step 2, θ_d (rad) is called the *dynamic contact angle*. When positive pressure is provided, the three phase boundary of liquid bridge increases, then the angle is called *advancing contact angle*. When negative pressure is provided, the three phase boundary of liquid bridge decreases, then the angle is called *receding contact angle*.

The distance between the tip of hollow cantilever and substrate at the instance the liquid bridge breaks h (m) in step 3 is called *break-up height*. The break-up height is obtained from Figure (2). There is a difference between the approach (blue) and retract (red) curves because when the tip retracts there is a liquid bridge connecting the AFM-tip and the substrate. Liquid bridge breaking occurs when the red line suddenly coincides with the blue line. The break-up height is calculated by subtracting the snap in position from the break-up position.

3. MODELING THE DOSING PROCESS

3.1 Flow rate

For uniform-viscous and incompressible Newtonian fluids with no body forces, the flow rate in a channel can be derived as in (Oh et al. (2012)) according to the electrical circuit analogy method:

$$Q = \frac{\Delta P}{R_H} \tag{1}$$

where Q (m^3/s) is the volumetric flow rate, ΔP (Pa) is the pressure difference, R_H (Pa $\cdot$ s/m^3) is the hydraulic resistance.
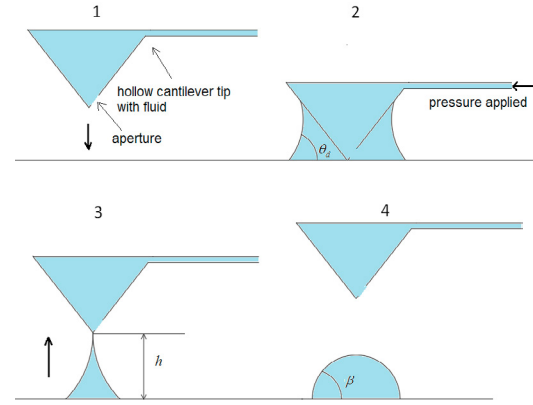

Fig. 1. Dosing process in four steps. These steps are repeated till the desired volume is achieved.
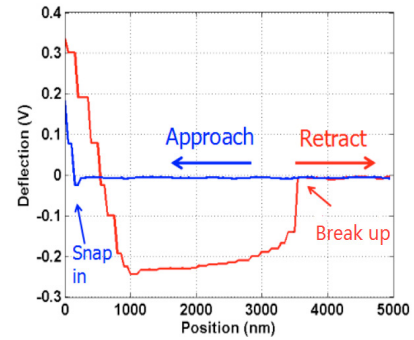

Fig. 2. The deflection of the cantilever with vertical position is shown. The blue line represents the cantilever approaching the substrate and the red line represents the cantilever retracting from the substrate.

The pressure of the liquid bridge will be calculated using the Laplace pressure formula. "The Laplace pressure is the pressure difference between the inside and the outside of a curved surface that forms the boundary between a gas region and a liquid region." (Butt et al. (2006)), which can be written as (Quéré et al. (2004)):

$$\Delta P = P_{inside} - P_{outside} = \gamma H \tag{2}$$

where P_{inside} (Pa) is the pressure inside the curved surface, $P_{outside}$ is the pressure outside the curved surface, H (1/m) is the curvature of the surface, which is sum of the two principle curvatures and γ (N/m) is the surface tension of the liquid.

3.2 Dynamic model

The scheme of the dosing process is shown in Figure 3. We define the following quantities:

$$\Delta P_p = P_p - P_{atm}, \quad \Delta P_m = P_m - P_{atm} \tag{3}$$

where P_p (Pa) is the pressure provided by pressure control system, P_m (Pa) is the pressure in the liquid bridge and P_{atm} (Pa) is the pressure of the atmosphere.

Then the flow rate Q can be expressed by the following differential equation with the hydraulic resistance R_H of the system:

$$\frac{dV}{dt} = Q = \frac{\Delta P_p - \Delta P_m}{R_H} \tag{4}$$

where, V (m^3) is the volume of the liquid bridge. Because ΔP_p is the system input, what needs to be determined is ΔP_m. In particular, since the output of the system is the volume of the liquid bridge, it is necessary to find a relation between ΔP_m and the volume. The model would become:

$$\frac{dV}{dt} = \frac{\Delta P_p - \Delta P_m(V)}{R_H} \tag{5}$$

The method to obtain the relation between pressure and volume is introduced in the following.
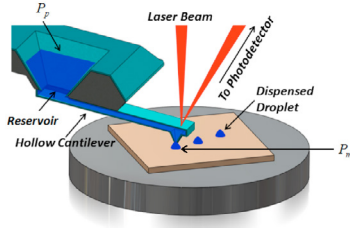

Fig. 3. The schematic of AFM-FP. The liquid is modelled as a uniform-viscous and incompressible Newtonian fluid (courtesy of Dr. Hector Hugo Perez Garza).

3.3 Young-Laplace equation

The profile of an axisymmetric liquid bridge between two solid surfaces can be described by solving Young-Laplace equation (Asay et al. (2010); Orr et al. (1975); Melrose (1966)). The tip of hollow cantilever can be approximated as cone. When the curvature of liquid bridge is negative, and the distance between the tip and substrate is D (see Figure 4), by solving the Young-Laplace equation, we can obtain:

$$2H_{mean}R_1 = \frac{1}{d}\{-\cos(\theta_1 + \psi) - \cos(\theta_2) - \frac{1}{k}[E(\phi_2, k) - E(\phi_1, k)] + \frac{1 - k^2}{k}[F(\phi_2, k) - F(\phi_1, k)]\} \tag{6}$$

where

$$k = (\frac{1}{1+c})^{1/2}$$
$$c = 4H_{mean}^2 R^2 \sin^2(\psi) - 4H_{meam}R\sin(\psi)sin(\theta_1 + \psi)$$
$$\phi_1 = -(\theta_1 + \psi) + 1/2\pi$$
$$\phi_2 = \theta_2 - 1/2\pi$$
$$d = \frac{y_1 + D}{R_1} = \frac{1}{\tan(\frac{\pi}{2} - \psi)}\sin\psi + \frac{D}{R_1}$$

H_{mean} is the mean of the two principle curvatures, which is $2H_{mean} = H$; R_1 is the radius of the circle which is tangent to the edge of the cone and pass through the point where the liquid bridge is connected to the cone. We define c_1 as:

$$2H_{mean}R_1 = HR_1 = c_1 \tag{7}$$

y_1 is the height of that point; θ_1 is the contact angle between the liquid and tip; θ_2 is the contact angle between liquid and substrate; F is the elliptic integral of first kind and E is the elliptic integral of second kind. Dynamic contact angle has a complex behavior for different liquids. For most liquids the advancing angle is the same when the

radius of droplet increases (Kwok and Neumann (1999)). The receding angle is more complex than the advancing contact angle. The receding contact angle can change with volume (Lam et al. (2002)). For small volumes, it is easy for the three phase boundary of liquid bridge to increase with increase in volume (Korhonen et al. (2013)). When considering dispensing process via hollow cantilever (for small volume), the angles θ_1, θ_2 (advancing contact angles) in (6) can be treated as constant values, and the distance between the tip and substrate D is zero. As a result (6) becomes an equation with the only variable $H_{mean}R_1$. So c_1 is constant in this condition.

As for the aspirating process, because θ_1 and θ_2 may not be constant, c_1 may change with volume and time.
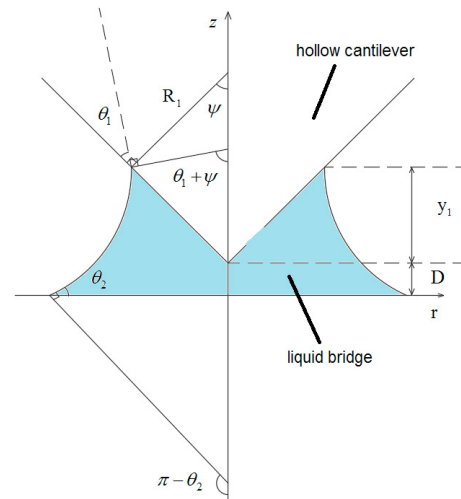

Fig. 4. Liquid bridge between a cone and plane.

If the distance D between the tip and substrate is not zero, c_1 will change when the volume changes. As for large volume of liquid bridge, there are three situations, which is shown in Figure 5.

In the situation (a), the distance D is small, but R_1 and y_1 are large. In the situation (b), the distance D is large, while R_1 and y_1 are small. In the situation (c), D, R_1 and y_1 are large. Because $d = \frac{y_1 + D}{R_1}$, in the situation (a), the part $\frac{D}{R_1}$ can be neglected, d can be approximated as the situation when the distance D is zero.

In the situation (b), D is much larger than R_1 and y_1. The relation between HR_1 and the ratio of $\frac{D}{R_1}$ is shown in the Figure 6 where $\theta_1 = 20°$, $\theta_2 = 20°$ and $\psi = 35°$. We can see when the distance D becomes larger HR_1 becomes smaller and changes slowly. So in this situation HR_1 can be treated as a small value near zero.

In the situation (c), because R_1, y_1 and D are very large, so when there is small increase of liquid bridge, just small increase happens in y_1 and D_1. d can be treated as constant. According to equation (6), HR_1 is constant when θ_1, θ_2 and ψ do not change. So we can conclude when the volume of liquid bridge is very large and the change of volume is small, even if distance D is not zero, c_1 can be treated as constant (not the same in different situations).
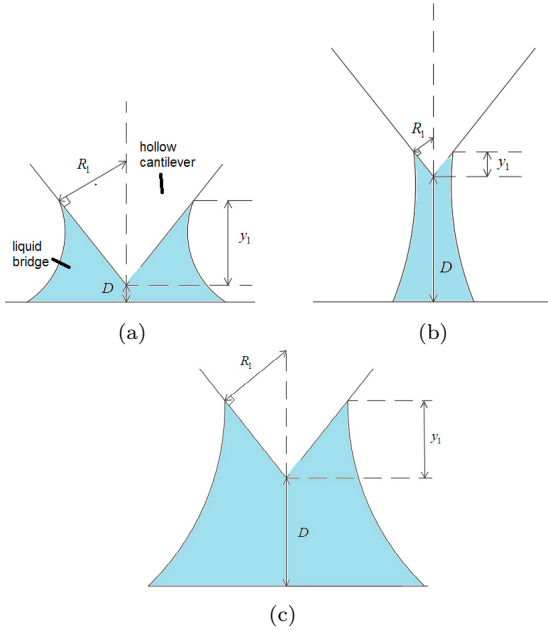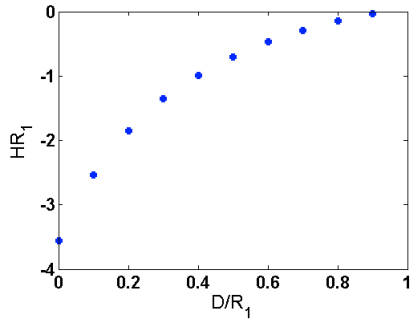
(a)   (b)

(c)

Fig. 5. Three situations of large liquid bridge.

Fig. 6. The relation between HR_1 and $\frac{D}{R_1}$ when $\theta_1 = 20°$, $\theta_2 = 20°$ and $\psi = 35°$.

When θ_1, θ_2 and ψ are constant, the volume V of the liquid bridge between the cone and plane can be calculated as:

$$V = c_2 R_1^3 \qquad (8)$$

where c_2 is the constant defined as:

$$c_2 = \int\limits_{\pi-\theta_2}^{\theta_1+\psi} \frac{\pi}{(2c_1)^3} \left(\sin^2(x) - 2\sin(x)(\sin^2(x) + c)^{1/2} \right.$$
$$\left. + \sin^2(x) + c \right) \left(\sin(x) - \frac{\sin^2(x)}{\sqrt{(\sin^2(x)) + c}} \right) dx \qquad (9)$$
$$- \frac{1}{3}\pi \frac{\sin^4 \psi}{\cos \psi}$$

According to (2) (7) and (8), the ΔP_m in model (5) can be calculated as:

$$\Delta P_m = \gamma c_1 \sqrt[3]{\frac{c_2}{V}} \qquad (10)$$

So the model becomes:

$$\frac{dV}{dt} = \frac{\Delta P_p - \gamma c_1 \sqrt[3]{\frac{c_2}{V}}}{R_H} \qquad (11)$$

4. METHODS TO MEASURE VOLUME AND CONTACT ANGLE

4.1 Volume Computation

In equation (8), the method gives the relation between the volume and R_1. But R_1 cannot be measured. To control the dosing process, the liquid volume has to be measured. The volume can be measured according to the break-up height.

The volume of the liquid V_h is calculated based on the shape of the liquid bridge at the break-up instant, as shown in Figure 7. The model assumes that the radius r of the liquid bridge is constant. If the contact angle θ (when the liquid bridge breaks) is known, the volume can be calculated as:

$$V_h = \pi \left\{ \frac{2h^3}{\cos^2 \theta} - \frac{h^3}{3} - 2\frac{h^3}{\cos^3 \theta} \left(\frac{1}{2} \cos\theta \sqrt{1 - \cos^2 \theta} + \frac{1}{2} \sin^{-1}(\cos\theta) \right) \right\} \qquad (12)$$
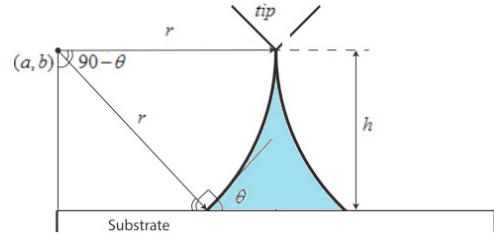

Fig. 7. A schematic picture of the event just before the liquid bridge breaks from the cantilever tip.

4.2 Contact angle measurement

The contact angle θ (Figure 7) at the break up instant is an important parameter to calculate the volume. However, it is hard to measure at the micro-scale; for this reason we measure in the macro-scale before gravity effects the droplet shape.

The device uses a dispensing needle to dispense liquid on the substrate and a camera to capture the image of the liquid bridge. The contact angle θ can be obtained by an image analysis software. The working principle of the software is to approximate the 2-D boundary shape of the liquid bridge with the arc of a circle: the contact angle is obtained by using the approximated circle and the substrate.

5. EXPERIMENTAL RESULTS

5.1 Dispensing on hydrophilic surface

To verify the model of the dosing process in equation (11), we first dispensed 5% glycerol on bare silicon substrate, where the contact angle was 32°. The droplet was too large, leading to no break-up occurring because of the limitation of the piezoelectric z-stage. To get useful data

in this situation, cantilever was made to contact with the liquid bridge and the tip need not have to be in contact with the substrate surface. Then it was observed that the volume increases with time. Two experiments were done, one was the distance between tip and substrate being small, the other was for large distance. No pressure was applied externally. The volume change with time can be obtained by considering the volume being proportional to the cube of the ratio between the diameter of the liquid bridge w_2 and the width of the cantilever w_1 (see Figure 10(a)):

$$ra = (\frac{w_2}{w_1})^3 \qquad (13)$$

The value of the volume at the ending of each experiment was obtained by using the droplet remained on the substrate after break-up, which is shown in Figure 8. The volume of the droplets is 2.75×10^4 fL and 1.9×10^4 fL. The larger one is in the condition when the distance between tip and substrate is small and the smaller one is in the condition when the distance between the tip and substrate is large. By using ra and droplet volume, we can calculate the volume of liquid bridge during dispensing process. The
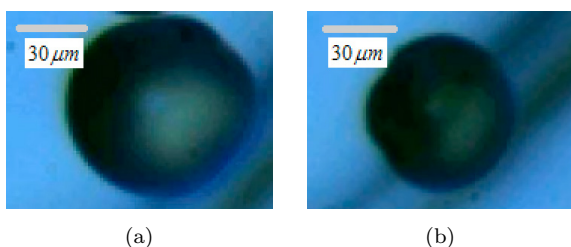
(a)　　　　　　　　　　(b)

Fig. 8. The droplet deposited on the substrate (after cantilever retracted) for a) small tip-substrate distance and b) large tip-substrate distance.

experiment results with different distance between the tip and substrate are shown in Figure 9 and 11 with red dots. The time 0 s means the start of recording images. Two of the recorded images in the two experiments are shown in Figure 10 and 12.

The evaporation rate is proportional to the radius of droplet (Birdi et al. (1989)). The volume of the liquid bridge is very large, so evaporation cannot be neglected.
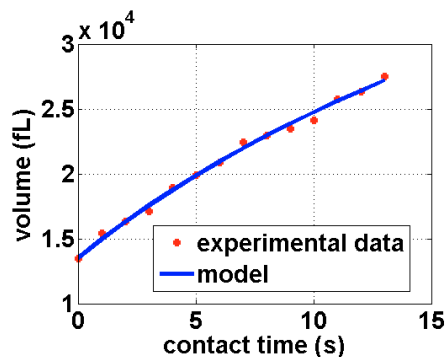
Fig. 9. Experimental result with small distance between the tip and substrate (the red dots are the experimental result, the blue dots are the result of fitting with the model (14)).
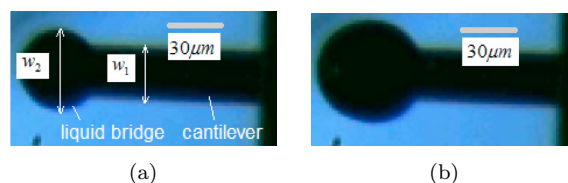
(a)　　　　　　　　　　(b)

Fig. 10. The dispensing process for small tip-substrate distance. a) Initial image when dispensing started (t=0) b) Final image when dispensing saturated (t=13s).
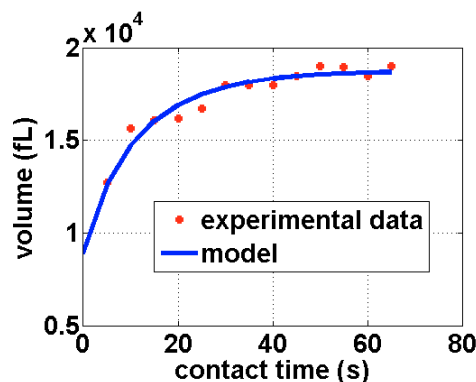
Fig. 11. Experimental result with large distance between the tip and substrate (the red dots are the experimental result, the blue line is the result of fitting with the model (14)).
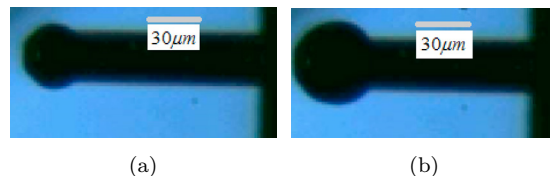
(a)　　　　　　　　　　(b)

Fig. 12. The dispensing process for large tip-substrate distance. a) Initial image when dispensing started (t=0) b) Final image when dispensing saturated (t=65s).

The evaporation rate should be proportional to the cube root of volume V. So the model (11) is changed to:

$$\frac{dV}{dt} = \frac{\Delta P_p - \gamma c_1 \sqrt[3]{\frac{c_2}{V}}}{R_H} - c_3 \sqrt[3]{V} \qquad (14)$$

c_3 is the parameter related to the evaporation rate. It can be seen that the model can match the data well with VAF 98.54% and 97.46% for the two experiments. The value of parameter $\frac{\gamma c_1 \sqrt[3]{c_2}}{R_H}$ obtained in the first experiment is $-0.2647 \times 10^{-18.667}$ m^4/s and c_3 is $0.0806 \times 10^{-9.33}$ m^2/s. For the second experiment, $\frac{\gamma c_1 \sqrt[3]{c_2}}{R_H}$ is $-0.2499 \times 10^{-18.667}$ m^4/s and c_3 is $0.1644 \times 10^{-9.33}$ m^2/s. When the distance between the tip and substrate increases, the volume increase speed decreases, which can be explained by (14), the absolute value of $c_1 \sqrt[3]{c_2}$ decreases when the d in equation (6) increases. And the interface area between liquid and vapor increases at certain liquid volume, which increases c_3.

5.2 Dispensing on functionalized surface

In this experiment, hollow cantilever with smaller aperture size was used, and the silicon substrate was func-
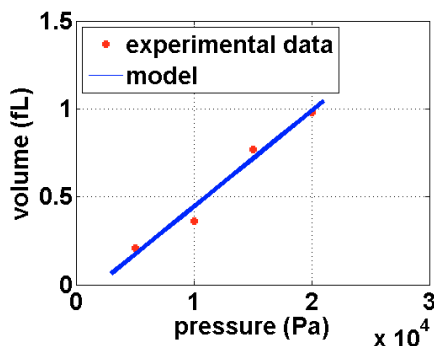
Fig. 13. Droplet volumes of 5% glycerol solution with varying pressure on funtionalized surface (De Gruiter (2015)).

tionalized by octyltrichlorosilane, to make the surface hydrophobic. The receding contact angle measured was about 50.5°, pressure control system provided 5000 Pa, 10000 Pa, 15000 Pa and 20000 Pa with the same contact time (0.5 s). And the volume was calculated according to equation (7) by using the break-up height. The result is shown in Figure 13. It can be seen that the relation between volume and pressure is almost linear. The reason is that when the substrate becomes more hydrophobic, the absolute value of $c_1\sqrt[3]{c_2}$ decreases because of the increase of θ_2 in equation (6), $\gamma c_1 \sqrt[3]{\frac{c_2}{V}}$ can be neglected in (14). And because the volume V in (14) changes in a very small range, the evaporation part can be treated as constant, so the average volume shows linear relation with pressure provided with VAF 91.85%. The R_H obtained from the experiment data is 1.8382×10^{22} Pa $\cdot$ s/m^3. And the average variation of volume on different pressure is less than 0.06 fL.

6. CONCLUSIONS AND FUTURE WORK

The purpose of the work was to develop a dynamic model for dosing liquids via atomic force microscope with femto pipette. The dynamic model we proposed combines the Laplace pressure theory with the electrical circuit analogy. The resulting model can be expressed by equation (14). Validation of the proposed modeling approach with experimental data demonstrates that the VAF of the model is larger than 90%. The model can describe the dosing process on different substrates. However, when the surface is hydrophilic, the liquid that is dispensed can reach the scale 10^4 fL, which is too large to be measured by cantilever deflection curves because of the limited z-range of the vertical deflection piezos.

Future work includes the following: to verify whether the model is valid in the femto-litre range on a hydrophilic surface and small aperture size. A small aperture size means large hydraulic resistance and it will help to obtain small volume that can be measured by AFM deflection curves even on hydrophilic surface.

REFERENCES

Asay, D., De Boer, M., and Kim, S. (2010). Equilibrium vapor adsorption and capillary force: Exact laplace–young equation solution and circular approximation approaches. *Journal of Adhesion Science and Technology*, 24(15-16), 2363–2382.

Birdi, K., Vu, D., and Winter, A. (1989). A study of the evaporation rates of small water drops placed on a solid surface. *The Journal of physical chemistry*, 93(9), 3702–3703.

Butt, H.J., Graf, K., and Kappl, M. (2006). Liquid surfaces. *Physics and Chemistry of Interfaces*, 4–25.

De Gruiter, R.B.T. (2015). *Dosing of femto liter volumes using hollow cantilever AFM*. Ph.D. thesis, TU Delft, Delft University of Technology.

Elnashaie, S.S., Danafar, F., and Rafsanjani, H.H. (2015). From nanotechnology to nanoengineering. In *Nanotechnology for Chemical Engineers*, 79–178. Springer.

Fabié, L., Durou, H., and Ondarcuhu, T. (2009). Capillary forces during liquid nanodispensing. *Langmuir*, 26(3), 1870–1878.

Ghatkesar, M.K., Garza, H.H.P., Heuck, F., and Staufer, U. (2014). Scanning probe microscope-based fluid dispensing. *Micromachines*, 5(4), 954–1001.

Korhonen, J.T., Huhtamaki, T., Ikkala, O., and Ras, R.H. (2013). Reliable measurement of the receding contact angle. *Langmuir*, 29(12), 3858–3863.

Kwok, D.Y. and Neumann, A.W. (1999). Contact angle measurement and contact angle interpretation. *Advances in colloid and interface science*, 81(3), 167–249.

Lam, C., Wu, R., Li, D., Hair, M., and Neumann, A. (2002). Study of the advancing and receding contact angles: liquid sorption as a cause of contact angle hysteresis. *Advances in colloid and interface science*, 96(1), 169–191.

Melrose, J.C. (1966). Model calculations for capillary condensation. *AIChE Journal*, 12(5), 986–994.

OConnell, C.D., Higgins, M.J., Marusic, D., Moulton, S.E., and Wallace, G.G. (2014). Liquid ink deposition from an atomic force microscope tip: deposition monitoring and control of feature size. *Langmuir*, 30(10), 2712–2721.

Oh, K.W., Lee, K., Ahn, B., and Furlani, E.P. (2012). Design of pressure-driven microfluidic networks using electric circuit analogy. *Lab on a Chip*, 12(3), 515–545.

Orr, F., Scriven, L., and Rivas, A.P. (1975). Pendular rings between solids: meniscus properties and capillary force. *Journal of Fluid Mechanics*, 67(04), 723–742.

Quéré, D., de Gennes, P., Brochard-Wyart, F., and Reisinger, A. (2004). Capillarity and wetting phenomena: Drops, bubbles, pearls, waves.

van Oorschot, R., Garza, H.H.P., Derks, R.J., Staufer, U., and Ghatkesar, M.K. (2015). A microfluidic afm cantilever based dispensing and aspiration platform. *EPJ Techniques and Instrumentation*, 2(1), 1.